Understanding the role of Al/Zr ratio in Zr-Al-Beta zeolite: towards the one-pot production of GVL from glucose

Marta Paniagua,[a]* Gabriel Morales,[a] Juan A. Melero,[a] Jose Iglesias,[a] Clara López-Aguado,[a] Nora Vidal,[a] Rafael Mariscal,[b] Manuel López-Granados,[b] Irene Martínez-Salazar[b]

[a] Chemical and Environmental Engineering Group. Universidad Rey Juan Carlos, C/Tulipán s/n. Móstoles. 28933 Madrid, Spain

[b] Energy and Sustainable Chemistry (EQS) Group. Institute of Catalysis and Petrochemistry, CSIC, Marie Curie 2, Campus de Cantoblanco. 28049 Madrid, Spain

Abstract

The direct one-pot transformation of glucose into γ-valerolactone (GVL) can be accomplished by means of a cascade of reactions in which Brønsted acid-catalyzed transformations are combined with catalytic transfer hydrogenation (CTH) by using 2-propanol as sacrificial alcohol, avoiding the use of high-pressure hydrogen. Catalysts containing Zr Lewis acid sites have been successfully applied in CTH reactions while the acid-driven transformations can be preferentially promoted by Brønsted Al-related acidity. Here, we present the combination of Zr and Al as active sites within a BEA zeolite structure as catalyst, with the possibility of adjusting the Al/Zr ratio from ∞ (commercial H-Beta) to 0 (aluminium-free Zr-Beta), which show a scale of Brønsted/Lewis acid sites ratios. The Al/Zr ratio has a strong impact on the products distribution. As the Zr content increases, higher amount of GVL is obtained, leading to a maximum over the catalyst with high amount of Zr and low content of Al acid sites (Al/Zr=0.2). An increase of reaction temperature, as well as reaction time, allows an enhancement of yields towards the desired products, leading to a maximum yield towards GVL of 24 mol% over Zr-Al-Beta (2.0), and a maximum yield towards isopropyl lactate of 26 mol% over Zr-Beta at 190 °C.

Keywords: Zirconium, beta zeolite, bifunctional catalyst, cascade reaction, gamma-valerolactone

1. Introduction

Nowadays, fossil fuels (i.e. oil, coal, and natural gas) remain the main source for chemicals, materials and transportation fuels. Aside of their intrinsic non-sustainable nature due to their non-renewable character, the high dependence on such fossil resources leads to serious environmental, socio-political and economical concerns. These include a vast production of greenhouse gasses emissions promoting global warming, as well as geopolitical conflicts, local instabilities and fluctuations in the prices of energy. This situation makes necessary the implementation of policies aimed at replacing such non-renewable sources with sustainable alternatives [1–3]. In this sense, residual biomass, as a renewable feedstock, is a highly promising alternative to petroleum that can also be processed into value-added chemicals, fuels and materials. This is especially relevant for lignocellulosic biomass, the most abundant form of terrestrial biomass. Specifically, the use of waste lignocellulose, coming from pruning, harvesting activities, forestry or forest cleaning, lumber and wood-related companies, is gaining great interest.

Cellulose is the largest fraction of lignocellulosic biomass, corresponding to 35-50 wt.% depending on its origin, being a linear polysaccharide consisting of glucose monomers. In turn, glucose is the most important sugar platform for the production of many important chemically-derived bio-compounds, including γ-valerolactone (GVL), levulinic acid (LA), alkyl levulinates (LEV), and alkyl lactates (LAC) [4–7], among others. Furfural (FAL) has also been described as a possible product directly produced from hexoses such as glucose [8]. Among such biomass-derived molecules produced in a hydrolytic cellulosic biorefinery, GVL, as a renewable and versatile platform chemical, is one of the most appealing compounds due to its attractive physicochemical properties (low toxicity and biodegradability), as well as its potential as sustainable biofuel. Currently several applications as green solvent, food additives, precursor of gasoline and diesel fuels, intermediate for bio-polymers, etc. have already been proposed [9–13]. On the other hand, levulinic acid is a versatile platform molecule that can be further upgraded to produce a wide range of chemicals, polymers, fuel additives, agrochemicals, etc [2,14,15]. Alkyl levulinates can be used in various applications, such as plasticizing materials or solvents, odour substances in the perfume and flavour industries and as biofuel for diesel formulation [16,17]. Lactic acid is a versatile α-hydroxyl carboxylic acid that has a variety of applications ranging from food to pharmaceutical industries [18,19]. Furfural is also a promising platform molecule for the production of some valuable furan-based chemicals, such as furfuryl alcohol, tetrahydrofurfuryl alcohol, tetrahydrofuran, 2-methylfuran and methyltetrahydrofuran [20,21].

The catalytic conversion of cellulose and its derivatives into such value-added chemicals under homogeneous catalysis usually relies on the use of mineral acids, like sulfuric acid, which introduces environmental, handling, and corrosion concerns. As an alternative, heterogeneous acid catalysts exhibit important advantages including enhanced selectivity, easiness of handling, and possibility of recovery and reuse. On the other hand, most of the cellulosic biomass transformation processes involve several reaction steps with different catalytic requirements and reaction conditions. From a processing point of view, the direct conversion of carbohydrates over a multifunctional catalyst without separating intermediates from the reaction mixture is more attractive, as the overall investment and operation costs would be reduced. Heterogeneous catalysts allow the incorporation of different functionalities within the same material, something hardly possible in homogeneous catalysts.

Thus, the catalytic transformation of glucose into the above-described platform molecules over heterogeneous catalysts has been widely described in recent literature. For instance, levulinic acid production from glucose has been studied over zeolites, metal chlorides, solid superacid and hybrid catalysts [4,22–24]. The one-pot production of alkyl levulinates has also been tackled directly from C6 sugars using zeolite H-USY, $SO_4^{2-}/ZrO_2–Al_2O_3$, sulfated zirconia and a combination of H-USY and SnO_2 [5,25–28]. Furfural production from glucose can be accomplished by means of a retro-aldol condensation reaction catalysed by Lewis acid sites, transformation investigated over zeolites [8,29,30]. Conversion of various pentoses and hexoses into methyl lactate has also been demonstrated for the Sn-Beta zeolite [31]. The formation of methyl lactate from glucose comprises the isomerization of the aldose into the ketose, the retro-aldol condensation into trioses, and finally the isomerization of trioses to alkyl lactate. These steps are mainly catalyzed by Lewis acid sites [6].

In this context, our research group have recently reported the synthesis of bifunctional zirconium modified beta zeolites (Zr-Al-Beta), via dealumination and post-synthetic grafting of Zr. These bifunctional materials have been successfully used in the one-pot production of GVL starting from xylose, furfural and levulinic acid, in a cascade of transformations mediated by catalytic hydrogen transfer (CTH) reduction of carbonyl groups using 2-propanol as hydrogen donor [32–35]. In a step forward in this research, we have now studied the chemical valorization of glucose in 2-propanol towards GVL and other valuable compounds over Zr-Al beta zeolites, tuning the Al/Zr molar ratio from commercial Al-Beta (zirconium-free) to Zr-Beta (aluminium-free). Indeed, the one-pot production of GVL directly from glucose has been scarcely reported. The group of Cui et al demonstrated the efficient conversion of different carbohydrates, including glucose, into γ-valerolactone (GVL) over combined $H_3PW_{12}O_{40}$ and Ru/TiO_2 catalysts

under H_2 gas, highlighting the positive effect of oxygen-containing co-solvents (methanol, ethanol and 1,4-dioxane). However, in this case, two catalysts were used and high hydrogen pressure was necessary [7]. Therefore, here we present for the first time the one-pot production of GVL directly from glucose using a multi-functional catalyst such as Zr-Al-Beta, where the Zr/Al ratio appears as a key parameter driving the selectivity of the cascade of reactions. Moreover, catalysts reusability of the synthesized zeolites has been studied.

2. Experimental procedure

2.1 Synthesis of catalysts

Commercial Al-Beta zeolite (CP814C) was purchased from Zeolyst International. Zr-Al-Beta zeolites were synthesized following a two steps procedure previously described [33,36]. The method used for the synthesis of the collection of catalysts has been optimized for the synthesis of Zr-Al-Beta zeolite in our previous work [32], via dealumination and post-synthetic grafting of Zr in the tetrahedral vacancies generated in the zeolitic network, using $Zr(NO_3)_4$ as zirconium source and the optimum water concentration during the impregnation, which leads to the highest dispersion of Zr species. First, partial dealumination was carried out by treatment the commercial Al-Beta zeolite in HNO_3 solution in the concentration range 0.1-10 M (room temperature, 1h, 20 $mL \cdot g^{-1}$). Total dealumination was accomplished using more severe conditions (100 °C, 20 h, 20 $mL \cdot g^{-1}$). After filtration and washing with deionized water until neutral pH, the resulting materials were dried overnight (110 °C). Subsequently, the incorporation of zirconium was accomplished by aqueous impregnation by suspending the dealuminated Beta zeolite in deionized water (10 $mL \cdot g^{-1}$) followed by the addition of the appropriate amount of zirconium nitrate (IV) (Chemical Point). The resultant slurry was heated under vacuum to remove the water, dried overnight and calcined in air at 200 °C for 6 h (3 °C· min^{-1} heating ramp), and then at 550 °C for 6 h at the same heating rate. Three Zr-Al-Beta zeolites were synthesized and named Zr-Al-Beta (x), x denoting their Al/Zr molar ratio. The Al-free material synthesized was denoted as Zr-Beta, whereas the commercial Zr-free material was named as Al-Beta.

2.2 Catalysts Characterization

Elemental analysis of zeolites composition was determined by Inductively-Coupled Plasma-Optical Emission Spectroscopy (ICP-OES) with a Varian Vista AX apparatus to determine the zirconium and aluminium content of the modified zeolites. Textural properties of the catalysts were calculated from nitrogen adsorption-desorption isotherms, recorded at 77 K, using a Micromeritics TRISTAR 3000 system. Surface area values were calculated from isotherm data

using the B.E.T. method and total pore volume was taken at P/P_o = 0.975 single points. X-ray powder diffraction (XRD) patterns were collected in a Philips X-pert diffractometer using the Cu Kα line in the 2θ angle range from 5° to 60° (step size of 0.04°). Total acidity of zeolites was determined by means of temperature programmed desorption of NH_3 in a Micromeritics 2910 (TPD/TPR) equipment fitted with a TCD detector. FTIR measurements for diffuse reflectance infrared Fourier transform (DRIFT) were carried out on a Nicolet 5700 spectrometer fitted with Hg–Cd–Te cryodetector. Deuterated acetonitrile (CD_3CN) and pyridine (Py) were used as molecular probes to evaluate surface acidity, and the spectra were obtained by a reaction camera equipped with a temperature controller that allowed in situ thermal treatments (Harrick Scientific Products, NY) using a praying mantis as a mirror optical accessory. Before recording the DRIFT spectra, the materials were treated at 120 °C for 1 h under an argon flow (50 mL min^{-1}) to clean the surface. Argon flow saturated with the molecular probe, CD_3CN or Py, was passed through the sample until saturation. Removal of physisorbed molecules was performed by heating at 100 °C for 5 min (CD_3CN) and 120 °C for 1 h under Ar flow (Py). DRIFT spectra were obtained in the spectral range of 4000-650 cm^{-1} with a resolution of 4 cm^{-1} upon cooling the samples down to room temperature. X-ray Photoelectron Spectroscopy (XPS) measurements were obtained using a Specs Phoibos 150 9MCD photoelectron spectrometer.

2.3 Catalytic tests

Catalytic runs were performed in liquid phase in a stainless-steel stirred autoclave (500 mL) fitted with temperature control and a pressure gauge. Typically, 5.5 g of glucose (Sigma Aldrich 99 wt.%) were mixed with 1.5 g of catalyst and 100 mL of 2-propanol (Scharlab 98 wt.%). Decane (Acros organics >99 wt.%) was added as internal standard for analytical purposes in a concentration of 10 $g \cdot L^{-1}$. After sealing the reactor, stirring was fixed at 1000 rpm and a heating rate of 2.5 $°C \cdot min^{-1}$ was established. Samples of the reaction media were withdrawn periodically and filtered into a vial. Selected catalysts were tested in reaction in the temperature range of 150-190 °C.

Conversion of glucose was evaluated by HPLC analysis with a refractive index detector (Varian 356-LC), using a Hi-PLEX H+ column (7.7 x 300 mm, 8 µm). Reaction samples were also analysed by gas chromatography (Varian 3900) using a capillary column, ZB-WAX Plus (30 m x 0.25 mm, DF=0.25 µm), and FID detector. Compounds detected by GC included furfural (FAL, Sigma Aldrich 99 wt.%), 5-(hydroxymethyl)furfural (HMF, Sigma Aldrich 99 wt.%) and the corresponding 5-(isopropoxymethyl)furfural (IMF), levulinic acid (LA, Sigma Aldrich 98 wt.%) and the corresponding isopropyl levulinate (ILEV), gamma-valerolactone (GVL, Sigma Aldrich 99 wt.%)

and isopropyl lactate (IPL) as main reaction products. The identification of the above bioproducts was checked by GC-MS using a Bruker 320-MS GC Quadrupole Mass Spectrometer. Product quantification was based on a previous calibration of the analysis unit with standard stock solutions of pure commercially available chemicals using n-decane as internal standard. Catalytic results are shown in terms of either conversion of glucose (X_{GLU}) or yields towards the different products (Y_i). The normalized selectivity, incorporating only identified products, was also evaluated (S_i). The definitions of these parameters are as follow:

$$X_{GLU} = \frac{Reacted\ mole\ of\ glucose}{Initial\ mole\ of\ glucose} \times 100$$

$$Y_i = \frac{Formed\ mole\ of\ i}{Initial\ mole\ of\ glucose\ \times\ stoichiometric\ coefficient} \times 100$$

$$S_i = \frac{Formed\ mole\ of\ i}{Total\ formed\ moles\ of\ identified\ products} \times 100$$

3. Results and discussion

3.1 Catalysts characterization

Different Zr-Al-Beta catalysts were synthesized, tuning the Al/Zr molar ratio from ∞ (commercial Al-Beta) to 0 (Zr-Beta). Table 1 summarizes the concentration of HNO_3 solution used during the dealumination step, as well as the physicochemical properties of the parent Al-Beta and modified Zr-Al-Beta zeolites. Elemental composition of the synthesized catalysts was determined by ICP-OES. Al/Zr atomic ratio have been adjusted through the severity of the dealumination process, and the subsequent incorporation of Zr species. Thus, a collection of Zr-Al-Beta materials with Al/Zr atomic ratios in the range of 0.0 to 1.4 have been obtained.

Table 1. Physicochemical properties of the parent Al-Beta and modified Zr-Al-Beta zeolites: composition, textural properties and acid properties.

Catalyst	HNO_3[a] (mol·L^{-1})	Composition[b]				Textural properties		Acid properties		
		% Al	% Zr	Si/Al	Al/Zr	BET area[c] (m^2g^{-1})	V_p[d] (cm^3g^{-1})	Acid sites loading[e] (mmol H^+g^{-1})	T_{max}[f] (°C)	B/L ratio[g]
Al-Beta	-	2.0	-	22	∞	600	0.33	0.40	333	0.56
Zr-Al-Beta (1.4)	0.1	1.1	2.7	38	1.41	560	0.32	0.34	307	0.52
Zr-Al-Beta (0.5)	1.0	0.6	3.8	69	0.55	570	0.33	0.25	294	0.31
Zr-Al-Beta (0.2)	6.5	0.4	5.2	117	0.23	530	0.30	0.29	265	0.17
Zr-Beta	10	0.04	5.2	1154	0.02	520	0.31	0.13	264	0.04

[a] Acid concentration during dealumination treatment. [b] % Al, % Zr (wt.); Si/Al, Al/Zr (atomic ratios) measured by ICP-OES. [c] Surface area calculated by the B.E.T. method. [d] Total pore volume recorded at $P/P_0 = 0.975$. [e] Acid sites loading analysed by NH_3-TPD.[f] Temperature of the maximum desorption of NH_3 analysed by NH_3-TPD. [g] Brønsted/Lewis acid sites ratio determined by FTIR using pyridine as molecular probe, as reported in ref. [37].

In order to check the preservation of the zeolitic network after the synthesis procedure, textural properties of the materials were studied by means of XRD and nitrogen adsorption-desorption isotherms (Fig. ESI-1). For all the materials, characteristic type 1-isotherms of microporous materials were obtained, with high N_2 adsorption at low relative pressures ($P/P_0 < 0.2$). The differences between them are not very relevant, implying similar textural properties. Hence, this indicates that the parent zeolitic structure of Al-Beta is essentially preserved after the synthesis procedure, even for the harsher dealumination process (zeolite Zr-Beta). Textural properties obtained from the isotherms, as shown in Table 1, point out the effect of the synthesis procedure: BET surface area decreases slightly with the increasing of the acid treatment severity, leading to the smallest value for Zr-Beta; while total pore volume does not suffer noticeable changes among all the materials. Regarding the preservation of the crystalline structure, Fig. ESI-1 also shows the high-angle XRD patterns of Zr-Al-Beta modified zeolites, including the diffractograms corresponding to commercial Al-Beta zeolite and crystalline ZrO_2 (monoclinic phase) for comparison purposes. Parent Al-Beta zeolite shows the typical diffraction pattern of the family of zeolites with a BEA framework. Modified Zr-Al-Beta materials keep the same XRD signals, indicating that the crystalline structure is not significantly damaged during the acid dealumination. Even the Zr-Beta sample, subjected to the most severe conditions during the dealumination step (10 M HNO_3, 20 h and 100 °C), keeps the BEA structure of commercial Al-Beta. On the other hand, from the X-ray diffractogram, it can also be inferred whether the incorporation of Zr involves the formation of crystalline domains of zirconium oxide, also known as zirconia, forming aggregates of relatively large size. As can be seen, none of the prepared catalysts shows significant evidence of the characteristic diffractions of zirconia (included as a reference in the figure). Although the presence of zirconium oxide nanocrystals cannot be discarded, this is a strong indication of the good dispersion of the Zr species throughout the BEA structure.

To complete the characterization of the materials, their acid properties have been studied in terms of the amount and strength of the acid sites. The total acidity and temperature of the maximum ammonia desorption values from NH_3-TPD analysis are depicted in Table 1, being the profiles shown in Fig. ESI-2. As the amount of Al decreases in the materials, accompanied by an increase of the amount of Zr incorporated in the structure, the intensity of the NH_3 desorption signal gets gradually smaller. This means that the total acidity of the materials decreases with the aluminium content, so that the material with the highest number of acid centres is the commercial Al-Beta zeolite and the material that presents the lowest total acidity is the Zr-Beta material (with a negligible percentage of aluminium). Likewise, the strength of the acid centres

can be preliminary assessed from the temperature of the maximum desorption of NH_3, since the higher the temperature necessary for chemical desorption, the stronger the interaction between the acid centre and the probe molecule. Thus, the commercial zeolite Al-Beta exhibits the higher value, 333 °C, as compared with the temperatures corresponding to the rest of zeolites. In general, samples modified with Zr correspond to materials with a lower acidity and acid strength, as a consequence of the dealumination process, in comparison with the starting H-Beta zeolite. However, it should be noted that the probe molecule used in this characterization (ammonia) is especially indicated to evaluate acidity due to aluminium, but not so much for weaker acidity, mainly Lewis type, as that provided by zirconium species.

In order to further explore the nature of the acidity in these catalysts, as well as the ratio among Brønsted and Lewis acid sites (B/L), pyridine FT-IR experiments have been performed. Fig. 1a shows the spectra of adsorbed pyridine within the region of 1400-1600 cm^{-1} [38,39]. On the one side, the decrease in the intensity of the vibration band located at 1545 cm^{-1}, ascribed to the adsorption of pyridinium ion onto the Brønsted acid sites, shows that the lower the aluminium content, the lower the intensity of such band. On the other side, the signal centred at 1452 cm^{-1}, which is attributed to pyridine adsorbed onto Lewis acid sites, becomes more intense as the Zr content increases in the samples. Although semi-quantitatively, the integration of those characteristic features serves to provide a value for B/L ratio (Table 1), which accordingly decreases with the incorporation of Zr.

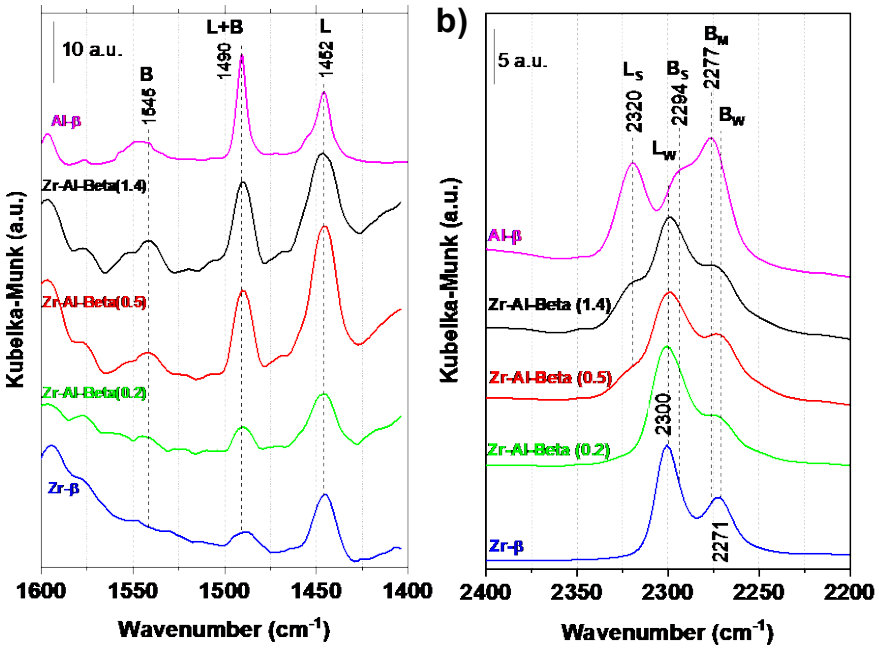

Fig. 1. (a) DRIFT spectra obtained for adsorbed pyridine and (b) DRIFT spectra obtained for adsorbed CD_3CN on the commercial Al-Beta zeolite and Zr-Al-Beta modified zeolites.

On the other hand, in line with the acidity characterization of the Brønsted and Lewis acid sites, deuterated acetonitrile has been found to be a suitable molecule for differentiating among acid sites of different strengths [40–42]. In previous studies devoted to Sn-USY, it has been shown that this probe molecule can be used for the semi-quantitative analysis of two types of Lewis acid sites [43]. The bands in the 2260-2340 cm^{-1} range are associated with the stretching of the bound C≡N group, attributed to weak Lewis Zr acid sites. Two peaks in this range are detected in Fig. 1b, centred at 2320 cm^{-1} and 2300 cm^{-1}, respectively assigned to strong and weak Lewis acid sites. In the same way, the Brønsted acid sites can be sorted by their strength, showing different wavelengths in the 2295-2270 cm^{-1} range in the FTIR spectrum. Going forward to the right in the IR spectrum, a decrease in the acid strength of the sites can be noticed. The IR peak detected at 2294 cm^{-1} is attributed to the strong Brønsted sites, while the peaks at 2277 cm^{-1} and 2271 cm^{-1} are supposed to be attributed to medium and weak Brønsted sites, respectively. For decreasing aluminium contents, Fig. 1b shows that the strong and medium Brønsted sites, and also the strong Lewis acid sites (2320, 2294 and 2277 cm^{-1}, respectively), get smaller until they disappear in aluminium-free Zr-Beta material. This can be attributed to the removal of, firstly, extra-framework octahedral aluminium and, secondly, structural tetrahedral aluminium from the zeolite framework during the dealumination process. Fig. 1b also shows that the amount of weak Lewis acid sites (2300 cm^{-1}) increases with the Zr content in the sample, confirming that the synthesis procedure allows for the framework incorporation of a rather high amount of Zr atoms without the formation of large ZrO_2 bulk crystals [44]. Finally, the IR signal centred at 2270 cm^{-1} is conventionally ascribed to nitrile groups interacting with surface silanols, which are quite abundant in these materials as a consequence of the dealumination process. As expected, the intensity of this signal increases for harsher dealumination treatments, due to the generation of a higher population of Si-OH groups [45].

In order to determine if the Zr species have been incorporated into the zeolite framework by an isomorphic substitution of Al with Zr, each material was further characterized by means of XPS. The recorded XPS profiles for the different materials show a displacement of the doublet core level Zr 3d towards those assigned to bulk ZrO_2 (Fig. ESI-3). Both binding energies positions shift to lower values as the Zr content increases. Zr-Beta zeolite signals are especially close to ZrO_2 ones suggesting the formation of some amorphous ZrO_2 aggregates, which became more abundant at the highest Zr loading.

3.2 Catalysts screening for glucose transformation and reaction network

The synthesised Zr-Al-Beta zeolites were first evaluated in the glucose transformation in the presence of 2-propanol. As a starting point, the catalysts were tested under reaction conditions

previously optimized for a different monosaccharide, xylose, in a previous work (8 h, 170 °C, 15 $g_{CAT} \cdot L^{-1}$; 2-propanol : Glucose = 40 : 1 (mol)) [32]. Fig. 2 shows the molar normalized selectivity of interesting identified products after reaction and the carbon balance for each material.

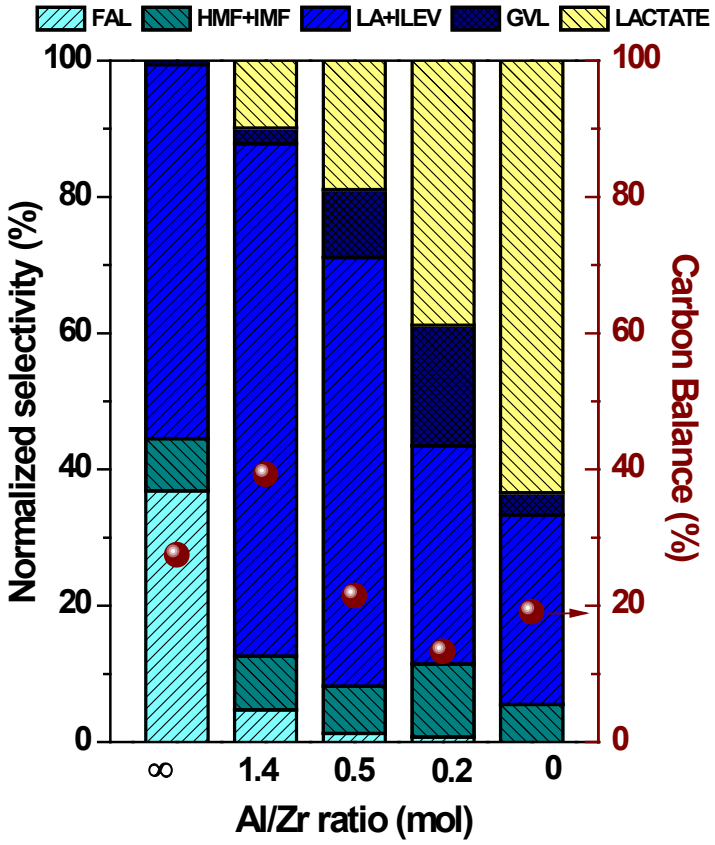

Fig. 2. Normalized selectivity (mol%) and carbon balance (mol%, as the ratio of carbon in starting glucose quantified as target products) using Zr-Al-Beta catalysts with different Al/Zr atomic ratio. Reaction conditions: 8 h, 170 °C, 15 gCAT·L-1; 2-propanol : Glucose = 40 : 1 (mol). FAL = furfural; HMF = 5-hydroxymethyl furfural; IMF = 5-isopropoxymethyl furfural; LA = levulinic acid; ILEV = isopropyl levulinate; GVL = γ-valerolactone; IPL = isopropyl lactate.

The conversion of glucose (GLU) in alcohol media leads to a wide range of interesting products consisting of furfural (FAL), 5-(hydroxymethyl)furfural (HMF) and the corresponding 5-(isopropoxymethyl)furfural (IMF), levulinic acid (LA) and the corresponding isopropyl levulinate (ILEV), gamma-valerolactone (GVL) and isopropyl lactate (IPL) as main compounds. These products were identified by GC-MS (Figures ESI-4, 5, 6 y 7). It must be noted that glucose conversion was above 90% for all the experiments after 8 hours of reaction. However, as shown in Fig. 2, carbon balance is low for all the materials tested, which can be attributed to a large extent of side-reactions, mainly leading to the formation of humins.

In a similar way to that previously described for xylose, a sequence of reactions starting from glucose leads to the production of different interesting biomass-derived products, achieving GVL as the final product. In this case, the cascade of reactions begins with the isomerization of glucose into fructose, a reaction that occurs in the presence of catalysts with Lewis acidity [46]. Both hexoses, in alcoholic medium and in the presence of Brønsted acid sites, can be etherified to their respective ethers, and subsequently dehydrated to obtain HMF [47]. Likewise, this molecule may also undergo an etherification with 2-propanol to give IMF. Next, both methyl-furfurals can evolve via acid catalysis through ring opening to give LA and ILEV [48]. Finally, in the presence of Zr Lewis acid sites, the MPV reduction of the carbonyl group in LA/ILEV takes place to afford the corresponding 4-hydroxyester or reduced acid, which immediately lactonizates in the presence of acid sites to give the final product, gamma-valerolactone (GVL). Therefore, such a one-pot transformation from glucose to GVL requires of the collaborative action of Brønsted and Lewis acid sites, herein provided and tuned by the ratio Al/Zr within the zeolite beta structure.

In addition, the formation of isopropyl lactate (IPL) has been also detected after reaction. This product does not come from the described mechanism of GVL formation, and thus the existence of a side reaction must be considered. The proposed reaction pathway involves the retro-aldol condensation of the hexoses (glucose and/or fructose) or the corresponding isopropyl ethers, leading to the formation of trioses, glyceraldehyde and dihydroxyacetone. In subsequent reaction steps, glyceraldehyde can be transformed into isopropyl lactate [5,6,31,49]. This side reaction was also described in the transformation of xylose in the presence of H-USY zeolite [34], being ascribed to the presence of Zr Lewis acid sites. On the other hand, although in small quantities, surprisingly furfural have also been identified as a reaction product. Currently, furfural is produced from the dehydration of pentoses over acid catalysts whereas hexoses such as glucose preferentially undergo dehydration to form 5-HMF. However, some researchers found that furfural can be formed from hexoses during hydrothermal treatment, even in the absence of catalysts [8,29,30]. Several possible pathways for the transformation of glucose into furfural have been proposed in literature, depending on the catalytic system. One plausible proposal for acid beta zeolite is that glucose decomposes into a pentose precursor and formaldehyde, followed by the dehydration of the pentose precursor to yield furfural [50].

According to these preliminary catalytic results, the proposed reaction network for the catalytic transformation of glucose in the presence of 2-propanol over Zr-Al-Beta zeolites is depicted in Scheme 1. As shown, aside of the target final product GVL, a variety of biomass-derived

chemicals can be obtained, which can be both final products and platform compounds of industrial interest.

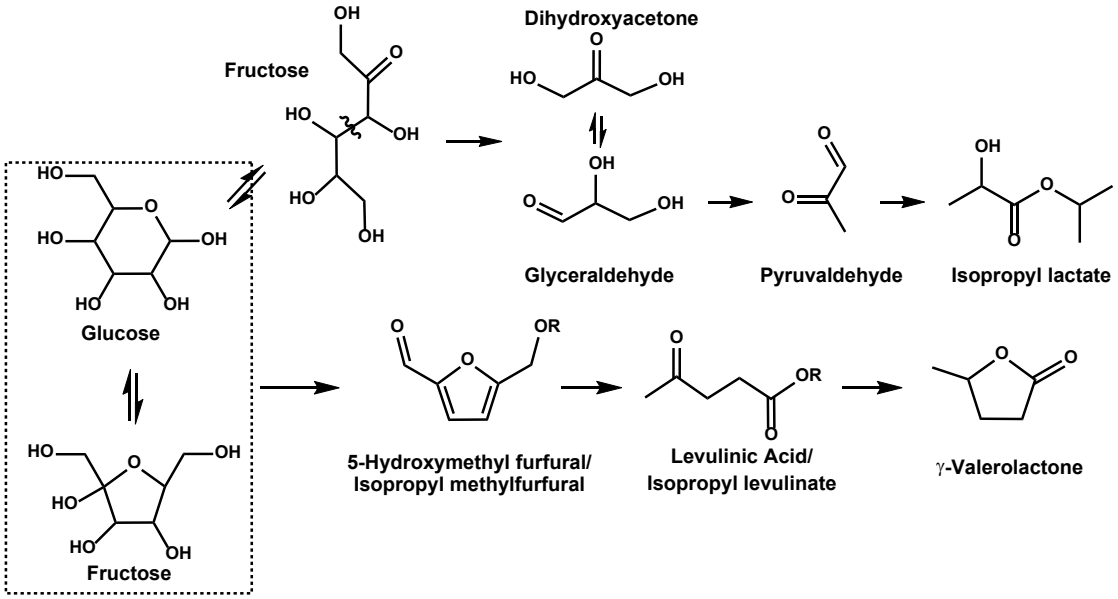

Scheme 1. Proposed reaction scheme for the transformation of glucose in 2-propanol over Zr-Al-Beta modified zeolites.

As depicted in Fig. 2, catalytic results show a strong dependence of the catalytic performance on the Al/Zr molar ratio. When using as catalyst the Zr-free commercial Al-Beta (Al/Zr ratio of ∞), which contains the highest proportion of strong Brønsted acid sites (Table 1, Fig. 1), the reactions requiring a strong acidity are clearly promoted. Thus, the products coming from the dehydration of hexoses (HMF/IMF), and the subsequent rehydration and ring-opening to form LA/ILEV, are observed. However, this catalyst is not able to promote the MPV hydrogen transfer step necessary to produce GVL, since the material does not contain the Zr Lewis sites needed to carry out the reduction of the carbonyl group. On the other hand, the production of furfural is favoured in the presence of this catalyst, in agreement with Cui et al. who suggested that Al-Beta benefits the formation of acyclic hexoses, being the transformation of cyclic hexoses to acyclic hexoses a step necessary for the subsequent C–C bond cleavage [8,29,30]. Finally, lactate formation has not been observed over this catalyst, in agreement with the absence of Zr sites promoting the retro-aldol condensation of sugars.

On the other hand, for the Zr-Al-Beta bifunctional materials, the products distribution varies significantly insofar as the Al/Zr ratio is gradually reduced. Thus, as zirconium content increases relative to Al content, the target cascade transformation of glucose into GVL is favoured, leading to a higher production of the intermediates LA/ILEV, and even reaching the final goal of

producing GVL in significant amounts. These results can be explained by the presence of a double functionality in the catalysts: Brønsted acid sites due to the remaining aluminium content, and zirconium Lewis acid sites, highly active in the MPV reduction of carbonyl groups. Interestingly, an Al/Zr molar ratio of 0.2 maximizes the direct formation of GVL from glucose. To the best of our knowledge, this is the first report on the direct one-pot production of GVL from glucose over a single bifunctional catalyst. Therefore, the presence of Zr in the adequate form and quantity is key to achieve such a goal. However, the parallel retro-aldol condensation of the sugar to produce isopropyl lactate is also clearly promoted by the presence of Zr sites (not seen over the zirconium free Al-Beta catalyst). In contrast, the production of furfural gradually diminishes with the Zr content as consequence of the decreasing of Al acid sites of high strength required for this reaction.

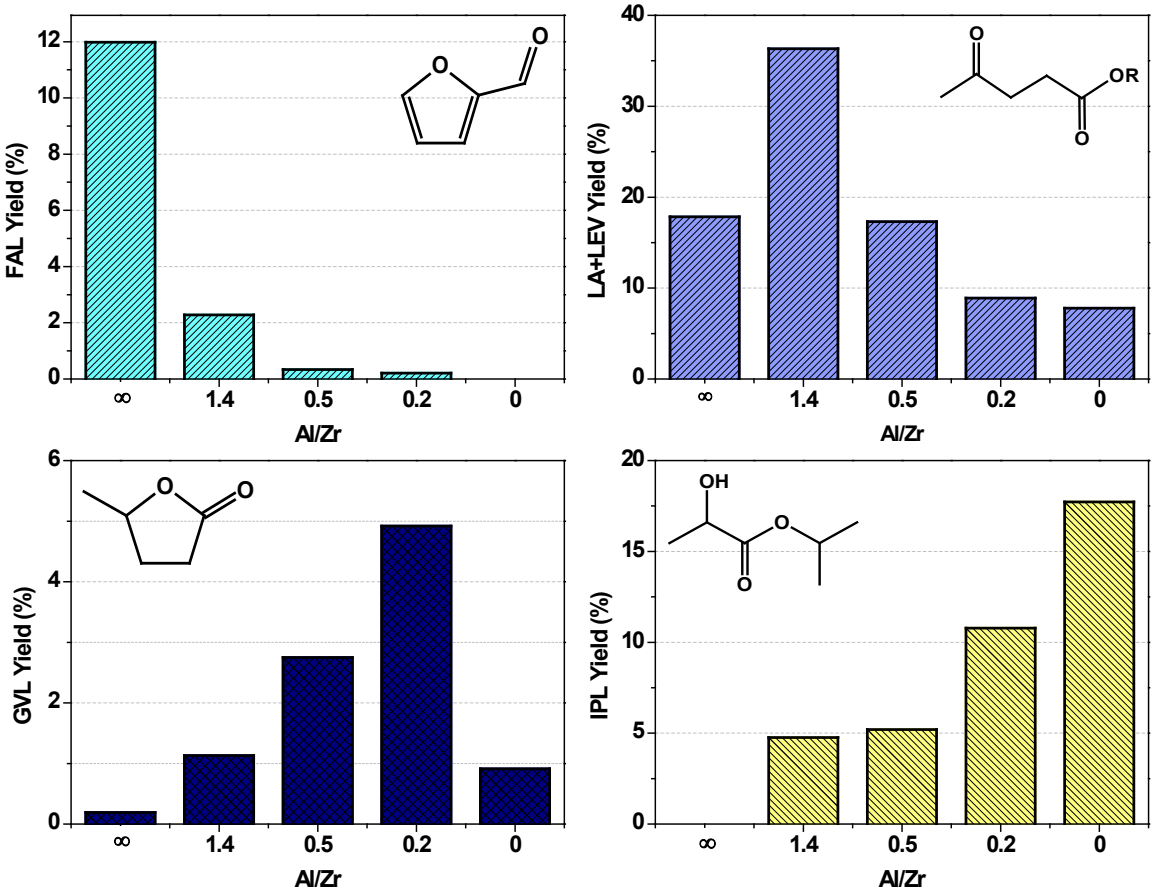

Fig. 3. Yields to the different products (FAL, LA/ILEV, GVL and IPL) in the one-pot transformation of glucose over commercial Al-Beta zeolite and Zr-Al-Beta modified zeolites. Reaction conditions: T = 170 °C. Catalyst loading = 15 $g \cdot L^{-1}$; 2-propanol : Glucose = 40 : 1 (mol); Reaction time = 8 h.

Fig. 3 shows the reaction results in terms of yields toward the different products as a function of the catalyst Al/Zr ratio. The catalyst providing the largest amount of furfural (up to 12 mol%) is the parent Al-Beta zeolite, while the dealuminated materials exhibit a dramatic reduction in the yield to FAL, down to 0.0 mol% for Zr-Beta. This is consistent with results previously reported in literature, wherein high yield of furfural was achieved successfully from cellulose catalyzed by Al-Beta zeolite [29]. The unique pore structure of Al-Beta seems to favour the special shape selectivity required for the furfural formation from glucose/fructose [8]. Replacement of Al sites by Zr species in the zeolitic framework decreases the activity of the catalyst in the cleavage of C-C bond and, therefore, reduces the amount of furfural formed. It is also important to note that furfural can be transformed in turn into GVL, as described in the literature [36,51–53]. Regarding the production of levulinic acid/levulinates from glucose, the literature reveals that a catalyst with both Brønsted and Lewis acidity is needed as this reaction involves various reaction steps: isomerization of glucose to fructose or glucosides to fructosides; dehydration of fructose/fructosides to HMF/IMF, and alcoholysis of IMF to ILEV [6]. Thus, the catalyst Zr-Al-Beta (1.4) seems to have the appropriate Al/Zr ratio for the most efficient conversion of glucose to alkyl levulinates, with some Zr sites to promote the isomerization reactions and enough strong acid sites in order to carry out the acid-driven reaction steps involved in this transformation. In contrast, the otherwise reduced presence of Al in this catalyst appears to inhibit the furfural production from glucose; and the amount of zirconium is not yet enough to carry out neither the final step of MPV reduction of LA/ILEV to yield GVL, nor the retro aldol condensation of the sugar into lactate. Focusing on the formation of GVL, zirconium-free Al-Beta zeolite (Al/Zr = ∞) leads to a negligible yield towards this compound, which indicates the necessity of using a catalyst that incorporates the second catalytic functionality (Zr sites) to fulfil the complete cascade of reactions. However, aluminium-free Zr-Beta zeolite (Al/Zr = 0) is not able either to promote the formation of GVL, in this case because the first steps of the cascade requiring strong acid sites cannot take place. Looking at the results obtained over the Zr-Al-Beta modified zeolites, as the ratio Al/Zr decreases in the Zr-Al-Beta modified zeolites, higher amount of GVL is obtained, leading to a maximum over the catalyst with an Al/Zr ratio 0.2 (approx. 5 mol%, under not optimized reaction conditions). Therefore, the composition of bi-functional Zr-Al-Beta zeolite can be tuned to promote the one-pot cascade reaction of glucose into GVL in 2-propanol. Unlike with xylose, the study of the transformation of glucose into GVL in a single reaction stage using a single bifunctional catalyst has not been described in the literature up to the best of our knowledge, hence this achievement is a clear advance in the field.

As previously described, besides the main cascade transformation of glucose into GVL, the parallel retro-aldol condensation of the sugar to produce isopropyl lactate (IPL) has also been detected. Fig. 3 shows that the incorporation of zirconium in the structure of the catalyst strongly enhances this reaction pathway. Zirconia-based materials have shown catalytic activity for these reactions [54] and we have also previously proven the existence of this transformation in the presence of Zr-containing zeolites, specifically, over Zr-USY zeolites [34]. In the present work, the results show that Al-Beta zeolite is not able to promote this reaction pathway since the strong aluminium sites lead preferentially to the dehydration of sugars/sugar ethers to HMF/IMF and then the rehydration to LA/ILEV. The progressive substitution of aluminium species by zirconium leads to an increase in IPL yield, confirming the key role on the catalytic behaviour of Zr sites. The highest yield to IPL, close to 20 mol%, was obtained over the aluminium-free Zr-Beta zeolite.

Finally, in all the catalytic experiments sugar conversion was above 90%. Taking into account the accumulated yields toward the identified products (Fig. 3), together with the formation of sugar ethers, it is clear the existence of a noticeable fraction of unaccounted products, mainly humins, which are not detected in the chromatographic analysis.

3.3 Reusability of the catalysts

Reusability of the catalysts was evaluated by means of two consecutive runs of the catalysts maximizing the yield of the compounds of interest described in the previous study: Al-Beta for furfural, Zr-Al-Beta (1.4) for LA/ILEV, Zr-Al-Beta (0.2) for GVL and Zr Beta for IPL. Catalysts were recovered by filtration after the first 8-hour reaction cycle and, once dried, were used again without any further treatment of regeneration in a second identical reaction cycle. Fig. 4 depicts the results in terms of products yield. As shown, no significant loss of catalytic activity is observed in GVL and IPL yields for Zr-Al-Beta (0.2) and Zr-Beta, respectively. On the other hand, for Al-Beta and Zr-Al-Beta (1.4), significant differences were found in the second catalytic cycle. These results show a clear deactivation of the active sites of the catalyst. It is important to note that the samples recovered after the first reaction cycle presented a dark colour, which increased as the aluminium content in the catalyst is higher, indicating the adsorption of organic compounds (desired products and humins).

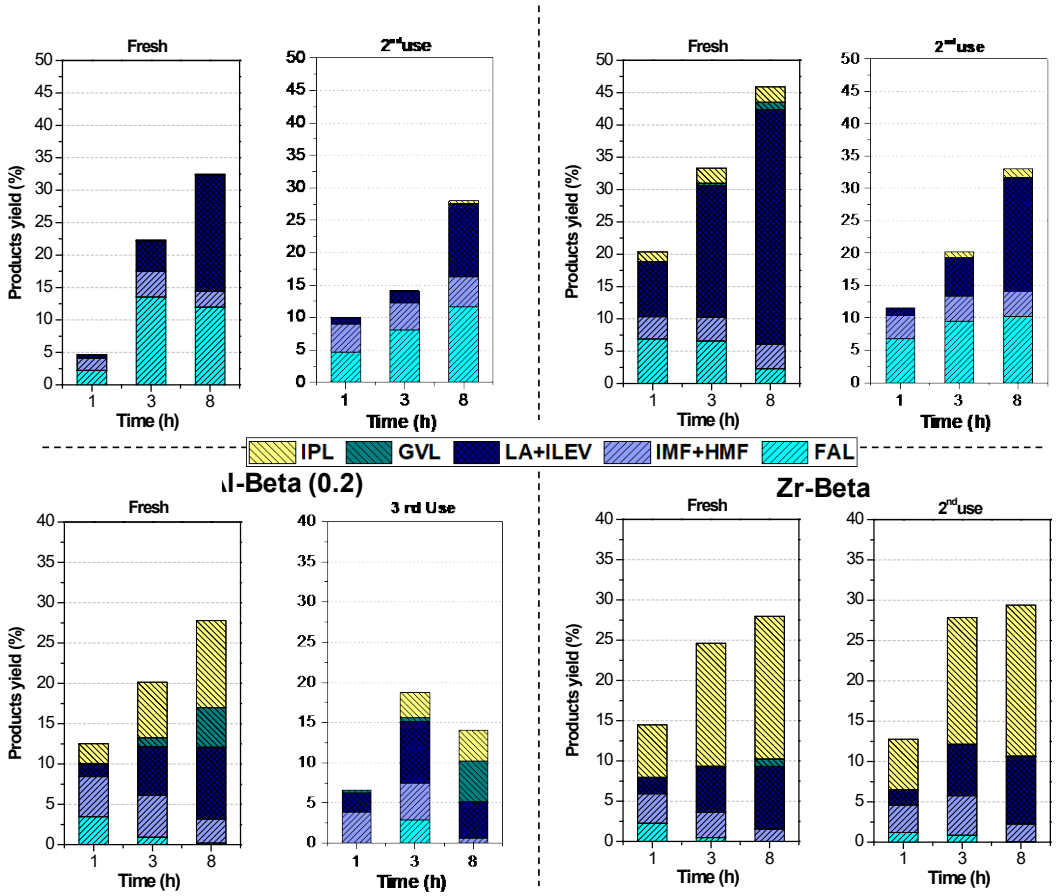

Fig. 4. Reutilization of Al-Beta, Zr-Al-Beta (1.4), Zr-Al-Beta (0.2) and Zr Beta. Yields to products (FAL, HMF+IMF, LA+ILEV, GVL and IPL) in the glucose transformation in two consecutives uses without any intermediate catalyst treatment. Reaction conditions: T = 170 °C. Catalyst loading = 15 $g \cdot L^{-1}$; 2-propanol : Glucose = 40 : 1 (mol); Reaction time = 8 h.

In order to determine the reason of the different behaviour among catalysts, TG analyses were carried out on the spent materials after the first reaction cycle (Fig. 5). For the solids with the highest aluminium contents, Al-Beta and Zr-Al-Beta (1.4), TG analyses indicate the presence of strongly adsorbed organic species, with desorption peaks around 400 °C, typical of strong acid sites such as Brønsted sites and hence more prominent in catalysts with high B/L ratios (Table 1). However, Zr-Al-Beta (0.2) and Zr-Beta, in which the most abundant catalytic sites correspond to Zr-sites, are not being affected in the same extent. As the Zr content in the modified Zr-Al-Beta catalysts increases, other types of degradation compounds are generated during the reaction and, although they are also adsorbed on the catalyst, they do not deactivate the active sites of the catalyst. This allows the catalyst to preserve the initial activity in the second run, even without any regeneration or washing treatment.

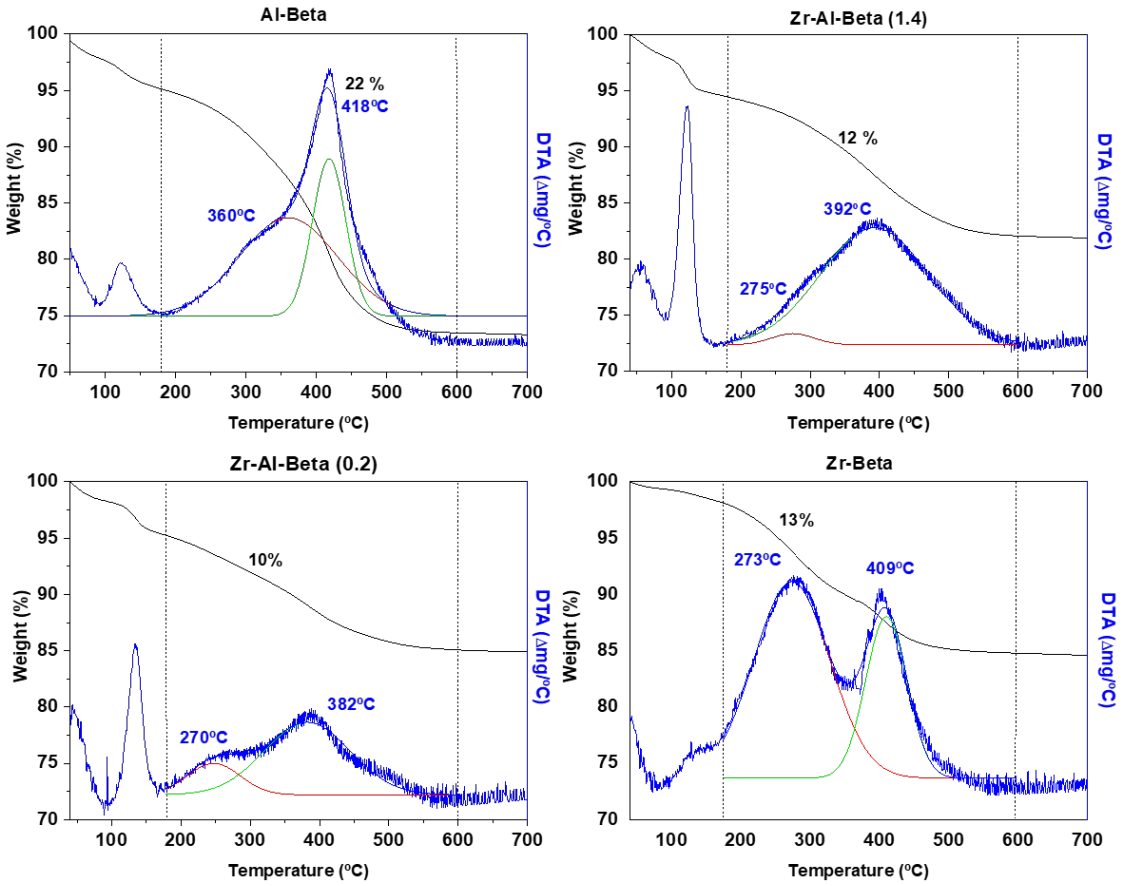

Fig. 5. TG analysis recorded for catalysts recovered after first reaction cycle in the transformation of glucose in 2-propanol. Reaction conditions: T = 170 ºC. Catalyst loading = 15 g/L; 2-propanol : Glucose = 40 : 1 (mol); Reaction time = 8 h.

Aiming to corroborate the hypothesis of deactivation by fouling, Al-Beta and Zr-Al-Beta (1.4) were used in a third catalytic cycle after a thermal treatment in air for 5 h at 550 °C, in order to remove the organic deposits from the catalysts surface (Fig. 4). In both cases, the catalytic activity and selectivity observed in the third use was similar to that obtained in the first use (Fig. ESI-8). In this sense, it is confirmed that the catalysts can be fully regenerated via calcination.

3.4 Effect of reaction time and temperature.

The effect to the reaction time and the temperature in the products yield was assessed in the range of 150-190 °C and 0-24 hours of reaction for those catalysts that have shown a better catalytic performance in terms of activity and reusability: Zr-Al-Beta (0.2) and Zr-Beta. The rest of the reaction conditions remained as in the previous study (catalyst loading = 15 g/L; 2-propanol : Glucose = 40 : 1). Fig. 6A shows the evolution with the time of the GVL yield in the glucose transformation over the Zr-Al-Beta (0.2) zeolite. When the temperature was reduced

down to 150 °C, the reaction rate became much slower and no GVL production was detected even after 24 hours of reaction. In contrast, increasing the temperature up to 190 °C introduced a high improvement in the GVL yield, as compared to 170 °C. The distribution products after 24 hours over the Zr-Al-Beta (0.2) zeolite is shown in Fig. 6B. Glucose conversion was almost total even for the lowest temperature. In addition, as the temperature rises, further progress is observed in the cascade of reactions, obtaining at 170 °C a GVL yield of 11 mol%. At this temperature, levulinic acid and isopropyl levulinate are still found in the reaction media, and they might be further converted into GVL at longer reaction times. At 190 °C, after 24 hours of reaction the highest yield of GVL, 24 mol%, was obtained. It is important to highlight that this value is the highest GVL yield obtained to date starting directly from glucose using a single bifunctional catalyst. Additionally, at 170 °C and 190 °C, a high yield to the products of retro-aldol condensation (17 %) is also observed. Surprisingly, the increase of temperature does not yield an enhancement of undesired side reactions, as the total yield towards products of interest rises for the highest temperature (Fig. 6B).

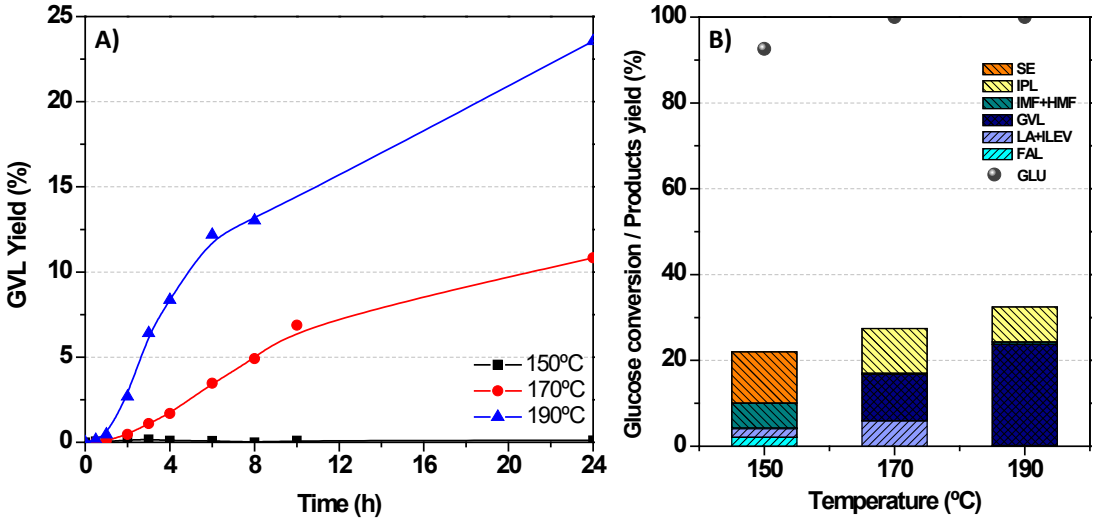

Fig. 6. A) GVL yield in the glucose transformation over the Zr-Al-Beta (0.2) zeolite. B) Glucose conversion and distribution of products after 24 hours over the Zr-Al-Beta (0.2) zeolite. SE, sugar ethers. Reaction conditions: Catalyst loading = 15 $g \cdot L^{-1}$; 2-propanol : Glucose = 40 : 1 (mol).

On the other hand, Fig. 7A shows the evolution with time of the IPL yield in the glucose transformation over the aluminium-free Zr-Beta zeolite. As shown, both the reaction time and temperature enhance the retro-aldol condensation, achieving the highest IPL yield at 190 °C and 24 h of reaction (ca. 26 mol%). Fig. 7B shows the products distribution of glucose transformation after 24 hours over Zr-Beta zeolite. Glucose conversion was almost complete for all three

temperatures. At 150 and 170 °C, the main products obtained were the ethers of sugars (SE), intermediate compound in the retro-aldol condensation pathway. As shown, as the temperature increases, the yield to isopropyl lactate is clearly enhanced, which confirms that the retro-aldol route requires high temperature conditions. On the contrary, such an increase in temperature also leads to a greater production of undesired degradation compounds (overall yield sharply diminishes down to 50 mol% from almost 90 mol%).

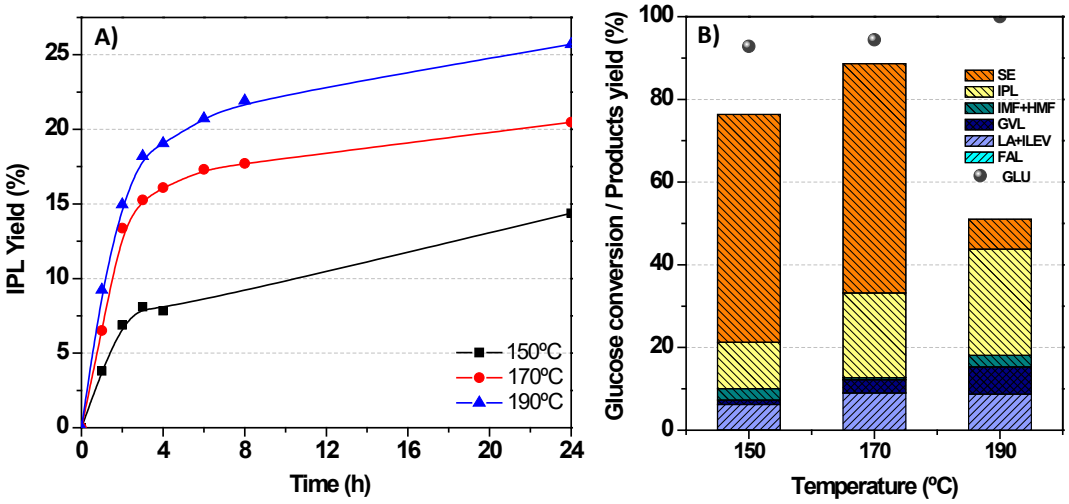

Fig. 7. A) IPL yield in the glucose transformation over the Zr-Beta zeolite. B) Distribution of glucose transformation products after 24 hours over the Zr-Beta zeolite. SE, sugar ethers. Reaction conditions: Catalyst loading = 15 $g \cdot L^{-1}$; 2-propanol : Glucose = 40 : 1 (mol).

Summarizing, the increase of the reaction temperature as well as reaction time allows completing the sequence of reactions and obtaining the maximum GVL yield, with a catalyst containing an Al/Zr ratio of 0.2, and without the enhancement of undesirable reactions (mainly those related with humins formation). On the other hand, the increase in the reaction temperature in the presence of the aluminium free catalyst, Zr-Beta, promotes the parallel retro-aldol condensation pathway leading to the preferential production of isopropyl lactate.

4. Conclusions

The one-pot production of GVL from glucose using a single Zr-Al-modified Beta zeolite catalyst has been demonstrated. The tuning of Al and Zr content in the synthetized zeolite allows settling the preferential reaction occurring in the one-pot transformation of glucose in alcoholic medium, and hence the final products distribution. The absence of Zr sites in parent Al-Beta

zeolite promotes mainly the formation of furfural whereas the gradual replacement of Al by Zr within the zeolitic framework enhances the formation of GVL. On the contrary, aluminium-free Zr-Beta zeolite catalyzes in a larger extent the formation of lactates through the retro-aldol condensation pathway. A partial deactivation of the catalyst with the highest aluminium contents is observed, related to the presence of strong acid sites more susceptible to fouling, though the catalytic performance is completely recovered after calcination. An increase of reaction temperature, as well as reaction time, allows an enhancement of yields towards the desired products, leading to a maximum yield towards GVL of 24 mol% over Zr-Al-Beta (2.0), and a maximum yield towards isopropyl lactate of 26 mol% over Zr-Beta at 190 °C.

Acknowledgements

The Spanish Ministry of Science, Innovation and Universities and the Regional Government of Madrid are kindly acknowledged for funding this research through the projects RTI2018-094918-B-C42, RTI2018-094918-B-C41, S2018/EMT-4344, and PEJD-2019-PRE_IND-15918. Clara López-Aguado acknowledges a FPI grant (BES-2015-072709) from the Government of Spain.

References

[1] J. Ma, S. Shi, X. Jia, F. Xia, H. Ma, J. Gao, J. Xu, J. Energy Chem. 36 (2019) 74–86.

[2] Z. Xue, Q. Liu, J. Wang, T. Mu, Green Chem. 20 (2018) 4391–4408.

[3] H. Li, A. Riisager, S. Saravanamurugan, A. Pandey, R.S. Sangwan, S. Yang, R. Luque, ACS Catal. 8 (2018) 148–187.

[4] N. Ya'Aini, N.A.S. Amin, S. Endud, Microporous Mesoporous Mater. 171 (2013) 14–23.

[5] J. Heda, P. Niphadkar, V. Bokade, Energy & Fuels 33 (2019) 2319–2327.

[6] L. Jiang, L. Zhou, J. Chao, H. Zhao, T. Lu, Y. Su, X. Yang, J. Xu, Appl. Catal. B Environ. 220 (2018) 589–596.

[7] J. Cui, J. Tan, T. Deng, X. Cui, H. Zheng, Y. Zhu, Y. Li, Green Chem. 17 (2015) 3084–3089.

[8] Y. Wang, X. Yang, H. Zheng, X. Li, Y. Zhu, Y. Li, Mol. Catal. 463 (2019) 130–139.

[9] A. Osatiashtiani, A.F. Lee, K. Wilson, J. Chem. Technol. Biotechnol. 92 (2017) 1125–1135.

[10] I.T. Horváth, H. Mehdi, V. Fábos, L. Boda, L.T. Mika, Green Chem. 10 (2008) 238–242.

[11] K. Yao, C. Tang, Macromolecules 46 (2013) 1689–1712.

[12] D.M. Alonso, S.G. Wettstein, J.A. Dumesic, Green Chem. 15 (2013) 584.

[13] J.Q. Bond, D.M. Alonso, D. Wang, R.M. West, J.A. Dumesic, Science (80-.). 327 (2010)

1110–1114.

[14] F.D. Pileidis, M.-M. Titirici, ChemSusChem 9 (2016) 562–582.

[15] B. Girisuta, H.J. Heeres, in: Springer, Singapore, 2017, pp. 143–169.

[16] A. Démolis, N. Essayem, F. Rataboul, ACS Sustain. Chem. Eng. 2 (2014) 1338–1352.

[17] D. Song, S. An, Y. Sun, Y. Guo, J. Catal. 333 (2016) 184–199.

[18] S. Li, W. Deng, Y. Li, Q. Zhang, Y. Wang, J. Energy Chem. 32 (2019) 138–151.

[19] F.A. Castillo Martinez, E.M. Balciunas, J.M. Salgado, J.M. Domínguez González, A. Converti, R.P. de S. Oliveira, Trends Food Sci. Technol. 30 (2013) 70–83.

[20] K.J. Zeitsch, The Chemistry and Technology of Furfural and Its Many By-Products, Elsevier, 2000.

[21] A. Mittal, S.K. Black, T.B. Vinzant, M. O'Brien, M.P. Tucker, D.K. Johnson, ACS Sustain. Chem. Eng. 5 (2017) 5694–5701.

[22] L. Peng, L. Lin, J. Zhang, J. Zhuang, B. Zhang, Y. Gong, Molecules 15 (2010) 5258–5272.

[23] H. Chen, B. Yu, S. Jin, Bioresour. Technol. (2011).

[24] D.W. Rackemann, W.O. Doherty, Biofuels, Bioprod. Biorefining (2011).

[25] C. Chang, G. Xu, W. Zhu, J. Bai, S. Fang, Fuel 140 (2015) 365–370.

[26] S. Saravanamurugan, A. Riisager, ChemCatChem (2013).

[27] L. Peng, L. Lin, J. Zhang, J. Shi, S. Liu, Appl. Catal. A Gen. 397 (2011) 259–265.

[28] G. Morales, A. Osatiashtiani, B. Hernández, J. Iglesias, J.A. Melero, M. Paniagua, D. Robert Brown, M. Granollers, A.F. Lee, K. Wilson, Chem. Commun. 50 (2014) 11742–11745.

[29] J. Cui, J. Tan, T. Deng, X. Cui, Y. Zhu, Y. Li, Green Chem. 18 (2016) 1619–1624.

[30] L. Zhang, G. Xi, Z. Chen, D. Jiang, H. Yu, X. Wang, Chem. Eng. J. 307 (2017) 868–876.

[31] M.S. Holm, Y.J. Pagán-Torres, S. Saravanamurugan, A. Riisager, J.A. Dumesic, E. Taarning, Green Chem. 14 (2012) 702.

[32] J.A. Melero, G. Morales, J. Iglesias, M. Paniagua, C. López-Aguado, K. Wilson, A. Osatiashtiani, Green Chem. 19 (2017) 5114–5121.

[33] B. Hernández, J. Iglesias, G. Morales, M. Paniagua, C. López-Aguado, J.L. García Fierro, P. Wolf, I. Hermans, J.A. Melero, Green Chem. 18 (2016) 5777–5781.

[34] C. López-Aguado, M. Paniagua, J. Iglesias, G. Morales, J.L. García-Fierro, J.A. Melero, Catal. Today 304 (2018) 80–88.

[35] G. Morales, J.A. Melero, J. Iglesias, M. Paniagua, C. López-Aguado, React. Chem. Eng. 4 (2019) 1834–1843.

[36] J.A. Melero, G. Morales, J. Iglesias, M. Paniagua, C. López-Aguado, Ind. Eng. Chem. Res. 57 (2018) 11592–11599.

[37] B. Hernández, J. Iglesias, G. Morales, M. Paniagua, C. López-Aguado, J.L. García Fierro, P. Wolf, I. Hermans, J.A. Melero, Green Chem. 18 (2016) 5777–5781.

[38] T. Barzetti, E. Selli, D. Moscotti, L. Forni, J. Chem. Soc. Faraday Trans. 92 (1996) 1401.

[39] G. Busca, Microporous Mesoporous Mater. 254 (2017) 3–16.

[40] J. Chen, J.M. Thomas, G. Sankar, J. Chem. Soc. Faraday Trans. 90 (1994) 3455–3459.

[41] R. Van Grieken, J.L. Sotelo, C. Martos, J.L.G. Fierro, M. López-Granados, R. Mariscal, Catal. Today 61 (2000) 49–54.

[42] M. Muñoz-Olasagasti, A. Sañudo-Mena, J.A. Cecilia, M.L. Granados, P. Maireles-Torres, R. Mariscal, Top. Catal. 62 (2019) 579–588.

[43] J. Iglesias, J. Moreno, G. Morales, J.A. Melero, P. Juarez, M. López Granados, R. Mariscal, I. Martinez-Salazar, Green Chem. 21 (2019) 5876–5885.

[44] V.L. Sushkevich, A. Vimont, A. Travert, I.I. Ivanova, J. Phys. Chem. C 119 (2015) 17633–17639.

[45] X. Yang, L. Wu, Z. Wang, J. Bian, T. Lu, L. Zhou, C. Chen, J. Xu, Catal. Sci. Technol. 6 (2016) 1757–1763.

[46] S. Saravanamurugan, M. Paniagua, J.A. Melero, A. Riisager, J. Am. Chem. Soc. 135 (2013) 5246–5249.

[47] L. Li, J. Ding, J.-G. Jiang, Z. Zhu, P. Wu, Chinese J. Catal. 36 (2015) 820–828.

[48] R.A. Sheldon, Green Chem. 16 (2014) 950–963.

[49] M.G. Manas, J. Campos, L.S. Sharninghausen, E. Lin, R.H. Crabtree, Green Chem. 17 (2015) 594–600.

[50] L. Zhang, G. Xi, Z. Chen, D. Jiang, H. Yu, X. Wang, Chem. Eng. J. 307 (2017) 868–876.

[51] H.P. Winoto, B.S. Ahn, J. Jae, J. Ind. Eng. Chem. 40 (2016) 62–71.

[52] M.M. Antunes, S. Lima, P. Neves, A.L. Magalhães, E. Fazio, F. Neri, M.T. Pereira, A.F. Silva, C.M. Silva, S.M. Rocha, M. Pillinger, A. Urakawa, A.A. Valente, Appl. Catal. B Environ. 182 (2016) 485–503.

[53] L. Bui, H. Luo, W.R. Gunther, Y. Román-Leshkov, Angew. Chemie - Int. Ed. 52 (2013) 8022–8025.

[54] P. Wattanapaphawong, P. Reubroycharoen, A. Yamaguchi, RSC Adv. 7 (2017) 18561–18568.